Optimal Load Control for Frequency Regulation under Limited Control Coverage

John Z. F. Pang, Linqi Guo and Steven H. Low
Department of Computing and Mathematical Sciences,
California Institute of Technology, Pasadena, CA, 91125

***Abstract*—Increasing renewable energy penetration imposes a problem as it proposes to solve one. In particular, generator-side control for frequency regulation becomes increasingly difficult due to slow reaction of generators to meet urgent needs, potentially caused by the stochastic nature of renewables. With increasing integration of smart appliances and other controllable loads which are able to sense, communicate and control, load-side control helps alleviate this problem which not only reacts fast but also localizes the disturbances. However, current methods for optimal load-side control requires full information and full controllability of nodes in the system. By framing the problem as an optimization problem and applying saddle-point dynamics, we obtain a control law that rebalances power and asymptotically stabilizes frequency after a disturbance. We generalize previous work [1], [2] to partial control over all nodes, which does not require full information over the network, yet still achieves secondary frequency control. We verify these results via simulation.**

I. Introduction

Frequency regulation aims to keep frequency of a power system close to its nominal value, which is typically 50 or 60 Hz. As supply and demand fluctuates, so does the frequency at each node, and such frequency deviation propagates over the network, leading to potential blackouts. In the past, generator-side control suffices for frequency regulation, and is typically classified under three stages at different timescales with distinct goals. Primary frequency regulation or frequency control, also known as droop control, is completely decentralized, and aims to bring the system to stabilization, i.e. suppressing the fluctuations, but not necessarily bringing the system back to nominal values, and often operate in the timescale of $10-30$ seconds. Secondary frequency control usually requires a central regulator which carefully modifies the set points of generation, in order to restore power interchanges and frequencies to their nominal values, and is usually observed from 30 seconds, but takes up till 15 minutes. Tertiary frequency control or economic dispatch is usually achieved to annihilate the mismatch and lighten the load on secondary frequency regulation.

A. Motivation for Limited Control Coverage

As renewable energy sources become increasingly utilized, fluctuation in supply increases too, due to the lack of predictability in yield of renewable energy sources such as solar or wind. While there have been improvements on the predictability of these renewables [3], this has mostly been insufficient for exact control, and thus frequency regulation still remains a relevant problem. It will continue to grow as a challenge in the advent of a new age of energy sources, as US states aim for 50% renewables by as early as 2030 [4], and also because alternatives such as battery storage programs are far from being cost-effective, with break-even costs estimated to be $197/kW [5].

Controllable loads, such as electric vehicle charging stations and smart household appliances, have been touted to have the ability to help decrease energy imbalance, and simulations together with real-world demonstrations highlight the potential of controllable loads [6]–[8]. However, in a large scale power grid, not every node have controllable loads of the capability to support frequency regulation, and participation in load-shedding may not have a 100% penetration rate across nodes geographically at all times, and therefore it is important to consider situations where the load control coverage is not full.

Indeed, popular controllable loads proposed in literature include smart appliances in households and electric vehicle charging stations. Households are found densely in some parts of the city and sparsely in others, and while placement of electric vehicle charging stations are increasingly dense, ones that are able to participate in frequency regulation may be limited by their geographical location and timing of participation. Furthermore, charging stations may also be limited by their current load demand and capacity, where it is possible that employees have to swap spots mid-day to provide charge to two or more cars per spot-day. In that case, new infrastructure have to be introduced, which is oftentimes not advantageous to the company. This subset of practical issues inhibiting full control coverage over all nodes of the power grid highlight the need for a more flexible control framework where not every node has controllable loads.

B. Literature Review

The use of primal-dual dynamics for control started out with the work of Kelly [9] and Low [10], [11] in network resources and [12] for stability of primal-dual dynamics. It has been in recent years transported to the power systems community for frequency control by [1] where Zhao's work [13] in identifying power system swing equations as a primal-dual dynamic sets the foundation for a series of other works in this area (e.g. [1], [2], [14]). In [1], primal-dual dynamics was used to implement distributed load side control for primary frequency regulation, in which they show that frequency deviations at each node convey exactly the right information about global power imbalance. Mallada *et al.* [2] extended the idea to also implement secondary frequency control, through the introduction of virtual line flows, which are exactly the same as real flows in steady state. Lastly, [14] further proposes a unified framework which integrates primary frequency control, secondary frequency control and congestion management. The primal-dual framework can also be used for economic dispatch or tertiary control, as in [15] and [16]. Jokić

[17] employs a similar method to attain real-time primary and secondary frequency control via setting of nodal prices instead of controllable loads. Recent noteworthy advances include passivity approaches for primary [18], [19] and secondary frequency regulation [20] with load-side participation, which offers increased flexibility over the use of Lyapunov functions, allowing generalization to higher order models. There is a much larger body of work on distributed frequency control (see e.g. [21]–[24] and references therein for recent examples) that does not employ the primal-dual framework.

Our work is most related to [1], [2], [14]. The key novelty in our work is that we do not assume that all nodes participate in load control, i.e. that the coverage of load control is limited, and only require communication with the neighbors of the controllable loads, which is specifically for the computation of line flow. We assume that there is an estimated global power imbalance, and show that (i) perfect estimation leads to a distributed control for secondary frequency control, and (ii) imperfect estimation leads to primary frequency control with bounds on the frequency deviations at steady state.

C. Summary

In this work, we focus on load-side participation for primary and secondary frequency control. In particular, assuming that the power or frequency imbalance can be reported through a distress signal in real-time, we show that a limited coverage of nodes participating in load control can cooperate to yield secondary frequency control. Our contribution in this work can be summarized as follows:

1) Primary Frequency Control under limited control coverage.
2) Secondary Frequency Control when perfect prediction of disruption in power supply is available.
3) Bounding the gap between nominal frequencies and stabilized frequencies when errors in such predictions are present.
4) Simulation of proposed control applied to a non-linear system with adversarially chosen control coverage. This demonstrates the effectiveness and robustness of our control design in real system.

II. Network Model & Preliminaries

In this section, we present the network model in our analysis and introduce notations used throughout the paper.

We adopt the model of Zhao et al. [1] and subsequently Mallada et al. [2]. The stark difference of our model from previous work is that we do not assume that all nodes admit controllable loads, are able to communicate, or have frequency dependent loads. We consider a power network described by the graph $\mathscr{G} = (N, E)$ where $N = \{1, \ldots, |N|\}$ is the set of buses and $E \subset N \times N$ is the set of transmission lines denoted by either e or (i, j) such that if $(i, j) \in E$, then $(j, i) \notin E$. We use the terms buses/nodes and edges/lines interchangeably in this paper. We also consider a communication graph $\mathscr{G}'_A$ with communication channels as edges linking a subset of buses A to their neighbors on the power network. This is a subgraph $\mathscr{G}'_A = (A, E')$ induced by the set of nodes $A \subseteq N$. Throughout our analysis, the following assumptions are made:

1) Lines (i, j) are lossless and characterized by their reactances x_{ij}.
2) Voltage magnitudes $|V_i|$ are time-invariant for all nodes $i \in N$, i.e. $|V_i(t_j)| = |V_i(t_k)|$ for all time $t_j,\ t_k$.
3) Reactive power injections to buses and reactive power flows are neglected.

We partition the buses as $N = G \cup L$ and use G and L to denote the set of generator and load buses respectively. Generator nodes $i \in G$ generates electrical power from mechanical power through AC generator and may also have loads. Load nodes $i \in L$ have only loads but no generators. The subset A of nodes N corresponds to active loads, i.e. nodes that participate in load control, and requires communication with their neighbors (the notation A here is intentionally repeated from the definition of the communication graph as the subset of nodes we need for the communication graph is exactly the load control coverage, and we henceforth drop the subscript A from $\mathscr{G}'_A$). We do not assume that all nodes have frequency sensitive loads, and identify the set of nodes with frequency sensitive load with F.

We further assume the system is three-phase balanced, and the frequency deviation from nominal values $\Delta\omega_i$ is small for all nodes $i \in N$ and the difference between phase angles $\theta_i - \theta_j$ are small across all links (i, j). We adopt a commonly used dynamic model (as in [25]), assuming coherency between internal and terminal voltage phase angles of generators, and model their dynamics by the following swing equation (1a). Correspondingly, load nodes require power balance as in (1b) and line flow deviations are modeled via linearized dynamics as in (1c). We consider these dynamics around an equilibrium point (ω^*, P^*), and all variables in (1) refer to its deviation from their corresponding nominal value. The notations are abused here for brevity of presentation, as in [1]:

$$M_i\dot{\omega}_i = P_i^m - (\mathbf{1}_{i\in A} d_i + \mathbf{1}_{i\in F}\hat{d}_i) - \sum_{e\in E} C_{ie}P_e, \quad \forall i \in G \tag{1a}$$

$$0 = P_i^m - (\mathbf{1}_{i\in A} d_i + \mathbf{1}_{i\in F}\hat{d}_i) - \sum_{e\in E} C_{ie}P_e, \quad \forall i \in L \tag{1b}$$

$$\dot{P}_{ij} = B_{ij}(\omega_i - \omega_j), \quad \forall (i, j) \in E \tag{1c}$$

where d_i denotes an aggregate controllable load and $\hat{d} := D_i\omega_i$ denotes an aggregate uncontrollable but frequency-sensitive load as well as damping loss at generator i and M_i is the generator's inertia. P_i^m is the mechanical power injected for generator buses $i \in G$, and is the aggregate power consumed by constant loads for load buses $i \in L$. P_{ij} is the line real power flow from i to j. C_{ie} are the elements of the incidence matrix $C \in \mathbb{R}^{|N|\times|E|}$ of the graph $\mathscr{G}$ defined as $C_{ie} = -1$ if $e = (j, i) \in E$, $C_{ie} = 1$ if $e = (i, j) \in E$ and $C_{ie} = 0$ otherwise. The incidence matrix C' for the communication graph is similarly defined. Finally we define $B_{ij} := 3\frac{|V_i||V_j|}{x_{ij}}\cos(\theta_i^n - \theta_j^n)$, where θ^n is the nominal phase angle of the node (and not the deviation). We refer the reader to Zhao et al. [1] for a detailed motivation of the model.

We are interested in the situation where the system is originally at an equilibrium, i.e. when $\dot{\omega} = \dot{P}_{ij} = 0$, and then the system is perturbed locally. Consequently, at time 0, there is a disturbance represented by the vector (of perturbations on the mechanical power injection) $P_m := (P_i^m, i \in G \cup L)$ that produces a power imbalance.

III. Design and Stability of Primary Frequency Control under Limited Control Coverage

In this section, we design a distributed control mechanism that rebalances the system while driving the frequency back to its nominal value, even in the setting where not all nodes participate in load control.

Following the footsteps of [1] and [2], we define an optimal load control (OLC) problem as follows:

$$\begin{aligned}\min_{d,\hat{d},P,R} \quad & \sum_{i\in A} c_i(d_i) + \sum_{i\in F} \frac{\hat{d}_i^2}{2D_i} \\ \text{s.t.} \quad & P_i^m - (\mathbf{1}_{i\in A} d_i + \mathbf{1}_{i\in F}\hat{d}_i) = \sum_{e\in E} C_{ie}P_e, \quad \forall i \in N \quad (2a) \\ & P_i^m + \hat{P}_i - d_i = \sum_{e\in E'} C'_{ie}R_e, \quad \forall i \in A \quad (2b)\end{aligned}$$

We would like to point out the subtle difference between our work and the work of [1] and [2] is that we no longer assume that the load control coverage is full, nor do we assume that every node is communicable and admit frequency sensitive loads. $\hat{P}_i$ is a constant which serves as an additional predicted contribution to the change in power and R_e is a virtual line flow. The purpose of including the former term will become clear in Lemma 2 and Section IV. We make the following assumptions:

Assumption 1: c_i's are strictly convex and twice continuously differentiable.

Assumption 2: OLC is feasible. This implies Slater's condition hold since all constraints in OLC are linear [26].

Let ν_i be the Lagrange multiplier associated with (2a) and λ_i for (2b). The dual of this problem can then be written as:

$$\max_{\nu,\lambda} \min_{d,\hat{d},P,R} \mathscr{L}(d,\hat{d},P,R,\nu,\lambda) \quad (3)$$

where $\mathscr{L}(d,\hat{d},P,R,\nu,\lambda)$ is:

$$\begin{aligned}&\sum_{i\in N}\Bigg[\nu_i P_i^m + \mathbf{1}_{i\in A}\left(c_i(d_i) - \nu_i d_i\right) \\ &+ \mathbf{1}_{i\in F}\left(\frac{\hat{d}_i^2}{2D_i} - \nu_i\hat{d}_i\right) + \mathbf{1}_{i\in A}\left(\lambda_i(P_i^m + \hat{P}_i - d_i)\right)\Bigg] \\ &+ \sum_{(i,j)\in E}\left((\nu_j - \nu_i)P_{ij} + \mathbf{1}_{(i,j)\in E'}(\lambda_j - \lambda_i)R_{ij}\right) \quad (4)\end{aligned}$$

By differentiation with respect to d_i and $\hat{d}_i$, we can obtain that the minimizer satisfies:

$$c_i'(d_i) = \nu_i + \lambda_i, \ \forall i \in A \text{ and } \hat{d}_i = D_i\nu_i, \ \forall i \in F \quad (5)$$

which suggests that the controllable load should be set, whenever possible, via:

$$d_i(\nu_i,\lambda_i) = (c_i')^{-1}(\nu_i + \lambda_i) \quad (6)$$

The maximum in (3) can only be attained if $\nu_i = \nu_j$ for all $i,j \in N$ and $\lambda_i = \lambda_j$ for all $i,j \in C_k'$ where C_k' is a connected component of the virtual network. Substituting these back into (4) implies that the dual of OLC can be equivalently written as the maximization of:

$$\begin{aligned}\Phi(\nu,\lambda) = \sum_{i\in N}\nu_i P_i^m + \mathbf{1}_{i\in A}(c_i(d_i(\nu_i,\lambda_i)) - \nu_i d_i(\nu_i,\lambda_i)) \quad (7) \\ -\mathbf{1}_{i\in F}\left(\frac{D_i\nu_i^2}{2}\right) + \mathbf{1}_{i\in A}\left(\lambda_i(P_i^m + \hat{P}_i - d_i(\nu_i,\lambda_i))\right)\end{aligned}$$

Lemma 1. *The function in* (7) *is separable, i.e.* $\Phi(\nu,\lambda) = \sum_i \Phi_i(\nu_i,\lambda_i)$*, where:*

$$\begin{aligned}\Phi_i(\nu_i,\lambda_i) = \nu_i P_i^m + \mathbf{1}_{i\in A}(c_i(d_i(\nu_i,\lambda_i)) - \nu_i d_i(\nu_i,\lambda_i)) \\ -\mathbf{1}_{i\in F}\frac{D_i\nu_i^2}{2} + \mathbf{1}_{i\in A}(\lambda_i(P_i^m + \hat{P}_i - d_i(\nu_i,\lambda_i)))\end{aligned}$$

Additionally, the Hessian of Φ_i *is given by:*

$$H_i = \begin{bmatrix} \mathbf{1}_{i\in A}(-d_i') + \mathbf{1}_{i\in F}(-D_i) & \mathbf{1}_{i\in A}(-d_i') \\ \mathbf{1}_{i\in A}(-d_i') & \mathbf{1}_{i\in A}(-d_i') \end{bmatrix}$$

where $d_i' = \frac{\partial d_i}{\partial \nu_i} = \frac{\partial d_i}{\partial \lambda_i}$.

Proof. Proof is direct and therefore left out. □

Therefore *strict concavity holds only when the node is active and also has frequency dependent loads*, as pointed out in [1].

When restricting to looking at only ν_i or λ_i alone, as long as the node is active, it is strictly concave in λ_i and if the node is either active or has frequency dependent loads, then Φ_i is strictly concave in ν_i.

Lemma 2. *Given a connected graph* $\mathscr{G} = (N,E)$*, fix the constants* $\hat{P}_i$*. Then there exist scalars* $\nu^*, \lambda_k^*, \ \forall k$ *(where* C_k' *is a connected component of the graph* $\mathscr{G}'$*) such that* $(d^*,\hat{d}^*,P^*,R^*,\nu^*,\lambda^*)$ *is primal-dual optimal for OLC and its dual if and only if* $(d^*,\hat{d}^*,P^*,R^*)$ *is primal feasible,* (ν^*, λ^*) *is dual feasible, and* (5) *and* (6) *hold.*

In addition, if we set $\hat{P}_i = \frac{\sum_{i\in(N-A)} P_i^m}{|A|}$ *(perfect prediction of the disruption in supply) in* (2b)*, we have that* $\nu^* = 0$*. In particular, secondary frequency control is attained.*

Proof. Since the OLC problem has only equality constraints, we use Karush-Kuhn-Tucker (KKT) conditions [26] to characterize the primal-dual solutions. In particular, $(d^*,\hat{d}^*,P^*,R^*)$ is primal-dual optimal if and only if:

1) Primal Feasibility: Constraints in OLC ((2))
2) Dual Feasibility: $\nu_i = \nu_j$ for all $i,j \in N$ and $\lambda_i = \lambda_j$ for all $i,j \in C_k$
3) Stationarity, i.e. Equations 5 & 6

Primal Feasibility is satisfied by assumption, Dual Feasibility amounts to $\nu_i = \nu^*$ for all $i \in N$ and $\lambda_i = \lambda_j$ for all $i,j \in C_k$, each connected component. Finally, Stationarity follows from Eq. 5 together with dual feasibility. This ends the proof for the first part of the lemma. For the second part of the lemma, note that summing up the modified second constraint, we have that:

$$\sum_{i\in A}(P_i^m - d_i^*) + \sum_{i\in N-A} P_i^m = 0 \quad (8)$$

and summing over the first constraint for all nodes, we get that:

$$\sum_{i\in N-A} P_i^m + \sum_{i\in A}(P_i^m - d_i^*) + \sum_{i\in F}\hat{d}_i^* = 0 \quad (9)$$

and subtracting one of the equations above from the other, we get that:

$$\sum_{i\in F} \hat{d}_i^* = 0 \Longrightarrow \nu^* = 0 \tag{10}$$

which concludes the proof. □

In the case where the prediction in the disruption of supply or global power imbalance is inaccurate, we are able to achieve primary frequency control and moreover, bound the deviation from frequency obtained with respect to the error of prediction:

Lemma 3. *Suppose for some $\varepsilon > 0$ we have $|\sum_{i\in A}\hat{P}_i - \sum_{i\in(N-A)} P_i^m| < \varepsilon$. Then:*

$$\left|\sum_{i\in F} \hat{d}_i^*\right| < \varepsilon \Longrightarrow |\nu^*| < \frac{\varepsilon}{\sum_{i\in F} D_i}$$

Note that in our setting of $\hat{P}_i$, we assume perfect prediction, but also apply a "fair" distribution of the information. This distribution of information (intuitively from (6)) affects the amount of the load control and can be distributed in a more optimal manner in the presence of either line flow limits or caps on controllable loads.

IV. Distributed Optimal Load Control

In this section, we focus on the case as is described in the latter part of Lemma 2, i.e. when we set $\hat{P}_i = \frac{\sum_{i\in(N-A)} P_i^m}{|A|}$, and devise a distributed optimal load-side control mechanism. We will assume that $F \neq \emptyset$.

Let

$$\begin{aligned}\mathscr{L}(P,R,\nu,\lambda) &= \min_{d,\hat{d}} \mathscr{L}(d,\hat{d},P,R,\nu,\lambda)\\ &= \mathscr{L}(d(\nu,\lambda),\hat{d}(\nu),P,R,\nu,\lambda)\\ &= \Phi(\nu,\lambda) - \nu^T CP - \lambda^T C'R\end{aligned}$$

where $\mathscr{L}(d,\hat{d},P,R,\nu,\lambda)$ as defined in (4), and $d(\nu,\lambda)$, $\hat{d}(\nu)$ as defined in (5). Similar to [1] and [2], we propose the following partial primal-dual algorithm:

$$\dot{\nu}_i = \zeta_i\left[P_i^m - \mathbf{1}_{i\in A}d_i - \mathbf{1}_{i\in F}D_i\nu_i - \sum_{e\in E} C_{ie}P_e\right],\ i\in G \tag{11a}$$

$$0 = P_i^m - \mathbf{1}_{i\in A}d_i - \mathbf{1}_{i\in F}D_i\nu_i - \sum_{e\in E} C_{ie}P_e,\ i\in L \tag{11b}$$

$$\dot{\lambda}_i = \eta_i\left[P_i^m + \hat{P}_i - d_i - \sum_{e\in E'} C'_{ie}R_e\right],\ i\in A \tag{11c}$$

$$\dot{P}_{ij} = \beta_{ij}(\nu_i - \nu_j) \tag{11d}$$

$$\dot{R}_{ij} = \alpha_{ij}(\lambda_i - \lambda_j) \tag{11e}$$

where its name comes from the fact that part of the dynamics (other than the dynamics on the load nodes $i\in L$) is the gradient descent step as in the primal-dual algorithm. Identifying ζ_i with M_i^{-1}, and β_{ij} with B_{ij}, the power system dynamics as described in (1a) can be interpreted as a subset of the partial primal-dual dynamics above, and we can identify the lagrange multiplier ν_i with ω_i. The parameters η_i and α_{ij} determines how much weight we want to place on information from the virtual variables.

Consider the Lagrangian of the dual of the OLC problem:

$$\begin{aligned}\mathscr{L}_D(\nu_G,\nu_L,\lambda,\pi) :&= \sum_{i\in N}\Phi_i(\nu_i,\lambda_i) - \sum_{(i,j)\in E}\pi_{ij}^N(\nu_i-\nu_j)\\ &\quad - \sum_{(i,j)\in E'}\pi_{ij}^C(\lambda_i-\lambda_j)\end{aligned} \tag{12}$$

To amend for the partiality of the primal-dual dynamics we used, consider the partial Lagrangian:

$$\mathscr{L}_D(P,R,\nu_G,\lambda) = \max_{\nu_L}\mathscr{L}_D(P,R,\nu_G,\nu_L,\lambda) \tag{13}$$

and by considering the same constraints as before, we get that the Lagrangian for the dual problem can be formulated in a way where ν_L takes on its unique maximizer value. By using the Envelope Theorem, we can then compute the partial derivatives of (13) with respect to the variables (P,R,ν_G,λ).

Indeed, partition the incidence matrix C (and correspondingly for C') between generator and load buses:

$$C = \begin{bmatrix} C_G \\ C_L \end{bmatrix}$$

and let

$$\Phi(\nu,\lambda) = \Phi_G(\nu_G,\lambda_G) + \Phi_L(\nu_L,\lambda_L)$$

where $\Phi_G(\nu_G,\lambda_G) = \sum_{i\in G}\Phi_i(\nu_i,\lambda_i)$ and $\Phi_L(\nu_L,\lambda_L) = \sum_{i\in L}\Phi_i(\nu_i,\lambda_i)$. We know that since we pick ν_L^* to be the maximizer, it satisfies:

$$\begin{aligned}&\frac{\partial\mathscr{L}_D}{\partial\nu_L}(P,R,\nu_G,\lambda,\nu_L^*(P,R,\nu_G,\lambda))\\ &= \frac{\partial\Phi_L}{\partial\nu_L}(\nu_G,\lambda,\nu_L^*(P,R,\nu_G,\lambda)) - (C_LP)^T = 0\end{aligned}$$

Therefore, applying the Envelope Theorem on (13) to compute the partial derivatives of $\mathscr{L}_D(P,R,\nu_G,\lambda)$ with respect to ν_G,λ,P and R, we get:

$$\begin{aligned}\frac{\partial\mathscr{L}_D}{\partial\nu_G}(P,R,\nu_G,\lambda) &= \left[\frac{\partial\mathscr{L}_D}{\partial\nu_G}(P,R,\nu,\lambda)\right]_{\nu_L^*(P,R,\nu_G,\lambda)}\\ &= \frac{\partial\Phi_G}{\partial\nu_G}(\nu_G,\lambda_G) - (C_GP)^T \qquad (14a)\\ \frac{\partial\mathscr{L}_D}{\partial\lambda_G}(P,R,\nu_G,\lambda) &= \frac{\partial\Phi_G}{\partial\lambda_G}(\nu_G,\lambda_G) - (C'_GR)^T \qquad (14b)\\ \frac{\partial\mathscr{L}_D}{\partial\lambda_L}(P,R,\nu_G,\lambda) &= \left[\frac{\partial\Phi_L}{\partial\lambda_L}(\lambda_L)\right]_{\nu_L^*(P,R,\nu_G,\lambda)}\\ &\quad -(C'_LR)^T \qquad (14c)\\ \frac{\partial\mathscr{L}_D}{\partial P}(P,R,\nu_G,\lambda) &= \nu_G^TC_L + \nu_L^*(P,R,\nu_G,\lambda)^TC_L \qquad (14d)\\ \frac{\partial\mathscr{L}_D}{\partial R}(P,R,\nu_G,\lambda) &= \lambda^TC \qquad (14e)\end{aligned}$$

and one can check that we end up with the same equations as with what is desired from (11).

Note that the resulting partial Lagrangian is exactly in the form of what Corollary 4.5 to Proposition 4.4 in [27] requires, which showed that primal dual dynamics are projected dynamical systems and establish that Carathéodory solutions exist and are unique, before employing the relevant invariance principle from [28] to show that primal-dual optimizers are

asymptotically stable under corresponding primal-dual dynamics. This implies that the proposed dynamics would be asymptotically stable.

We restate the above result from [27] for completeness:

Corollary 4. *For a C^1 function $F(x,z) : \mathbb{R}^n \times \mathbb{R}^m \to \mathbb{R}$, if*

1) *F is globally convex in x and linear in z,*
2) *for each $(x_*, z_*) \in Saddle(F)$, if $F(x,z_*) = F(x_*,z_*)$, then $F(x,z_*) \in Saddle(F)$,*

then $Saddle(F)$ is globally asymptotically stable under the saddle point dynamics and, moreover, convergence of trajectories is to a point.

C^1 functions are continuously differentiable functions and $Saddle(F)$ are the sets of saddle points of the function F. Precisely, to invoke the corollary, we need to show the following:

1) L continuously differentiable.
2) L globally concave in (ν_G, λ) and linear in P, R.
3) For every saddle point $(x^* = (\nu_G, \lambda)^*, z^* = (P^*, R^*))$ of L, if $L(x,z^*) = L(x^*,z^*)$, then (x,z^*) a saddle point too.

Referring to Equations 6,7 above, since c_i assumed to be continuously differentiable, the function L is continuously differentiable, satisfying the first condition. The function L, by plain inspection, is concave in ν_G, λ and is linear in P, R. Lastly, note that Slater's conditions are assumed to hold, and therefore saddle points are optimal and all optimal points are saddle points. Therefore, if another point obtains optimal solution, then it is a saddle point, as needed to be shown.

With the above results, we can state the main theorem of this work:

Theorem 5. *Assume the physical graph $\mathcal{G} = (N,E)$ is connected, $A \neq \emptyset$, $F \neq \emptyset$, and $L \subseteq F \cup A$. The system asymptotically converges to an equilibrium point where stabilization takes place.*

If in addition, an exact estimate $\hat{P}_i$ of the power step change is available, secondary frequency control can be attained in the converged state.

In the case of inaccurate predictions of the power step change, the performance of the dynamics can be bounded as:

$$|\nu^*| < \frac{\varepsilon}{\sum_{i \in F} D_i}$$

where ε is the error in prediction.

V. Numerical Illustrations

To demonstrate the performance of our load control to aid secondary frequency control, we apply our control design on the IEEE 39-bus New England interconnection test system. We include here the single line diagram of the 39-bus system, given in Fig. 1. There are 10 generators in the system and 29 load nodes, and unlike our analytical linear model, the simulation used adopts a more realistic nonlinear set-up, including e.g. nonlinear governor dynamics. The network parameters and initial stationary points were obtained from the Power System Toolbox data set [29].

In this simulation, we pick out a subset of nodes randomly for load control, and choose one node randomly (among the ones not chosen for load control) to add a step increase of 1pu (based on 100MVA) of its current load. We do not limit the amount of load control that the nodes can utilize, and illustrate that secondary frequency control can be attained. As suggested by previous related work [1], we use the disutility function for controllable loads $c_i(d_i) = 10d_i^2$.

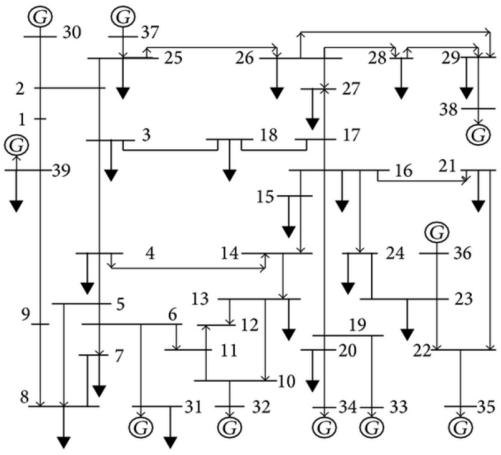

Fig. 1: Line diagram of the IEEE 39 bus system. In our simulations presented here, the load control cover nodes 1, 3, 30, 39 (top right) and the node experiencing the supply step change is node 35 (bottom left). We use this to demonstrate the ability to control loads even when controllable loads are limited in coverage and geographically located far away from the node experiencing disruption.

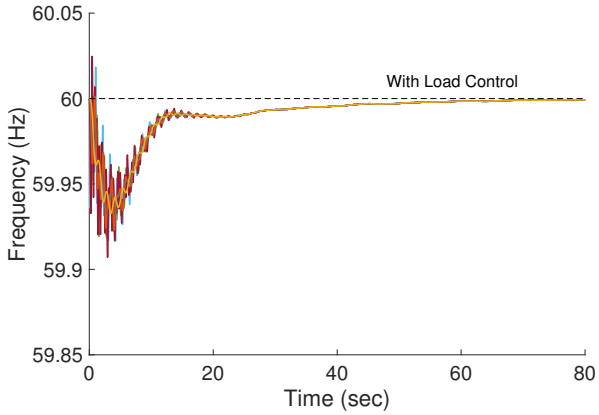

Fig. 2: Comparison of the system with proposed load control. Note that in this simulation, we only apply load control on 4 nodes and 1 node (located geographically far away from the load control coverage) experiences a step change in its supply. The system achieves secondary frequency control, compared to primary frequency control without load control.

A. Secondary Frequency Control under unlimited load control

As previously stated, nodes are chosen randomly for the controllable nodes and the disrupted node. As a motivating example, the results we present for illustration are for nodes 1, 3, 30 and 39, with the node experiencing disruption being node 35. With our control steps, we get the following dynamics as shown in Fig. 2. These nodes are chosen to explicitly illustrate

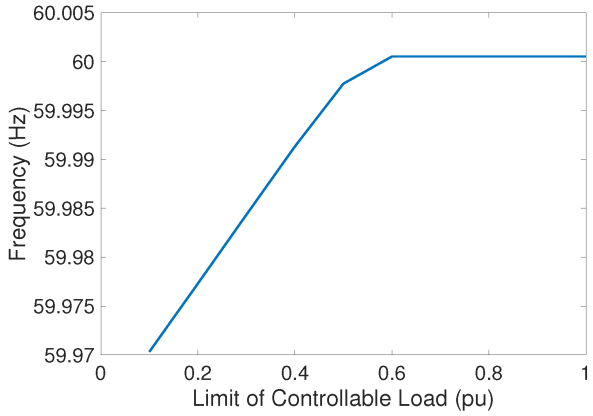

Fig. 3: Stabilized Frequency Value (i.e. Primary Frequency Regulation) as a function on the limit $\overline{d_i}$ of controllable loads d_i at nodes under limited control coverage. Observe as the limit on d_i passes a threshold of 0.6pu, Secondary Frequency Regulation is attained.

the ability to perform secondary frequency control even when the load control coverage is small, i.e. around 10%, and are not close to the disrupted node in the system, that nevertheless secondary frequency control is obtained. Simulations varying the proximity of load control coverage to the disrupted node suggests that the distance plays a part in the nadir of the frequency deviation and the time taken for convergence.

In comparison, we show the resulting dynamics without any load control. Note that governor dynamics also guide the system to primary frequency control and therefore, we notice that the system achieves primary frequency control. However, the time scale at which it achieves primary frequency control is out of the suggested time scale of 30s, which still suggests the necessity of load-side participation. This is pointed out in [1] previously, which showed a time improvement with load side control.

B. Effects of the size of controllable loads

In the previous subsection, simulation is done assuming controllable loads are able to take any load level. In practice, however, there is a feasible region where any controllable load can take value from, and therefore it is interesting to see the effects of having a limited size of the load.

The experiment results are illustrated in Fig. 3. In particular, regardless of the size of the controllable load, primary frequency control is always achieved. As we decrease capacity of controllable loads, the gap between the asymptotic frequency and its nominal value increases. Its impact is similar to having an inaccurate prediction of the power disruption, but the size of the controllable load cannot be negative, which could instead cause the system in certain cases to perform even worse than it would without any predictions.

VI. Conclusion & Future Work

In this work, we propose a control design for frequency control based on a linearized model of the swing equations. By exploiting the amenability of the primal-dual dynamics, part of the dynamics can be designed to match power system dynamics. The control steps and virtual variables are updated based on the values of the physical variables, which we leave for the system to compute (and we only need to measure). We prove that under some mild conditions, the system provably converges with an accurate prediction of the disruption of power, and bounds on the performances are provided with respect to inaccuracies in predictions.

We implement our control steps on a simulation involving non-linear dynamics, demonstrating the performance and robustness of our control design. An intuition to this robustness is our usage of the accurate measured physical variable to guide our control and virtual variables. We show that, even in a system where controllable loads are located geographically distant from the power disruption and with a limited load control coverage, the proposed control drives the system back to its nominal frequencies.

An observation made over the random simulations was that the proximity of the controllable loads to the power disruption affects the nadir of the frequencies and the time taken for nominal frequencies to be attained. As such, an interesting future direction would be to identify a relationship between the set of controllable loads, the resulting virtual network, the nadir of frequency dynamics and convergence time of the control. Another future direction is to seek good real-time estimates for P_i^m, and to better assign load control signals $\hat{P}_i$ (taking into account limits on loads) rather than the uniform manner we are proposing.

References

[1] C. Zhao, U. Topcu, N. Li, and S. Low, "Design and stability of load-side primary frequency control in power systems," *Automatic Control, IEEE Transactions on*, vol. 59, no. 5, pp. 1177–1189, 2014.

[2] E. Mallada, C. Zhao, and S. Low, "Optimal load-side control for frequency regulation in smart grids," in *Communication, Control, and Computing (Allerton), 2014 52nd Annual Allerton Conference on*. IEEE, 2014, pp. 731–738.

[3] J. Twidell and T. Weir, *Renewable energy resources*. Routledge, 2015.

[4] A. Olson, A. Mahone, E. Hart, J. Hargreaves, R. Jones, N. Schlag, G. Kwok, N. Ryan, R. Orans, and R. Frowd, "Halfway there: Can california achieve a 50% renewable grid?" *IEEE Power and Energy Magazine*, vol. 13, no. 4, pp. 41–52, 2015.

[5] T. Kiefer, "Caiso battery storage trial," 2017. [Online]. Available: http://tdworld.com/blog/caiso-battery-storage-trial

[6] D. Hammerstrom, R. Ambrosio, J. Brous, T. Carlon, D. Chassin, J. DeSteese, R. Guttromson, G. Horst, O. Järvegren, R. Kajfasz *et al.*, "Pacific northwest gridwise testbed demonstration projects," *Part I. Olympic Peninsula Project*, vol. 210, 2007.

[7] J. Lopes, F. Soares, and P. Almeida, "Integration of electric vehicles in the electric power system," *Proceedings of the IEEE*, vol. 99, no. 1, pp. 168–183, Jan 2011.

[8] M. Caramanis and J. M. Foster, "Management of electric vehicle charging to mitigate renewable generation intermittency and distribution network congestion," in *Decision and Control, 2009 held jointly with the 2009 28th Chinese Control Conference. CDC/CCC 2009. Proceedings of the 48th IEEE Conference on*, Dec 2009, pp. 4717–4722.

[9] F. P. Kelly, A. K. Maulloo, and D. K. Tan, "Rate control for communication networks: shadow prices, proportional fairness and stability," *Journal of the Operational Research society*, vol. 49, no. 3, pp. 237–252, 1998.

[10] S. H. Low, F. Paganini, J. Wang, S. Adlakha, and J. C. Doyle, "Dynamics of tcp/red and a scalable control," in *INFOCOM 2002. Twenty-First Annual Joint Conference of the IEEE Computer and Communications Societies. Proceedings. IEEE*, vol. 1. IEEE, 2002, pp. 239–248.

[11] M. Chiang, S. H. Low, A. R. Calderbank, and J. C. Doyle, "Layering as optimization decomposition: A mathematical theory of network architectures," *Proceedings of the IEEE*, vol. 95, no. 1, pp. 255–312, 2007.

[12] D. Feijer and F. Paganini, "Stability of primal-dual gradient dynamics and applications to network optimization," *Automatica*, vol. 46, no. 12, pp. 1974–1981, 2010.

[13] C. Zhao, U. Topcu, and S. Low, "Swing dynamics as primal-dual algorithm for optimal load control," in *Smart Grid Communications (SmartGridComm), 2012 IEEE Third International Conference on*. IEEE, 2012, pp. 570–575.

[14] C. Zhao, E. Mallada, S. Low, and J. Bialek, "A unified framework for frequency control and congestion management," in *Power Systems Computation Conference (PSCC), 2016*. IEEE, 2016, pp. 1–7.

[15] N. Li, C. Zhao, and L. Chen, "Connecting automatic generation control and economic dispatch from an optimization view," *IEEE Transactions on Control of Network Systems*, vol. 3, no. 3, pp. 254–264, 2016.

[16] L. Bai, M. Ye, C. Sun, and G. Hu, "Distributed control for economic dispatch via saddle point dynamics and consensus algorithms," in *2016 IEEE 55th Conference on Decision and Control (CDC)*, Dec 2016, pp. 6934–6939.

[17] A. Jokić, M. Lazar, and P. P. van den Bosch, "Real-time control of power systems using nodal prices," *International Journal of Electrical Power & Energy Systems*, vol. 31, no. 9, pp. 522–530, 2009.

[18] A. Kasis, E. Devane, C. Spanias, and I. Lestas, "Primary frequency regulation with load-side participation part i: stability and optimality," *IEEE Transactions on Power Systems*, 2016.

[19] E. Devane, A. Kasis, M. Antoniou, and I. Lestas, "Primary frequency regulation with load-side participation part ii: beyond passivity approaches," *IEEE Transactions on Power Systems*, 2016.

[20] A. Kasis, E. Devane, and I. Lestas, "Stability and optimality of distributed schemes for secondary frequency regulation in power networks," in *Decision and Control (CDC), 2016 IEEE 55th Conference on*. IEEE, 2016, pp. 3294–3299.

[21] Z. Wang, F. Liu, L. Chen, and S. Mei, "Distributed economic automatic generation control: A game theoretic perspective," in *2015 IEEE Power Energy Society General Meeting*, July 2015, pp. 1–5.

[22] T. L. Vincent, K. Poolla, S. Mohagheghi, and E. Bitar, "Stability guarantees for primary frequency control with randomized flexible loads," in *2016 American Control Conference (ACC)*, July 2016, pp. 2328–2333.

[23] L. Tang and J. McCalley, "Two-stage load control for severe under-frequency conditions," *IEEE Transactions on Power Systems*, vol. 31, no. 3, pp. 1943–1953, May 2016.

[24] P. ulc, S. Backhaus, and M. Chertkov, "Optimal distributed control of reactive power via the alternating direction method of multipliers," *IEEE Transactions on Energy Conversion*, vol. 29, no. 4, pp. 968–977, Dec 2014.

[25] A. R. Bergen, *Power systems analysis*. Pearson Education India, 2009.

[26] S. Boyd and L. Vandenberghe, *Convex optimization*. Cambridge university press, 2004.

[27] A. Cherukuri, E. Mallada, and J. Cortés, "Asymptotic convergence of constrained primal–dual dynamics," *Systems & Control Letters*, vol. 87, pp. 10–15, 2016.

[28] A. Bacciotti and F. Ceragioli, "Nonpathological lyapunov functions and discontinuous carathéodory systems," *Automatica*, vol. 42, no. 3, pp. 453–458, 2006.

[29] J. H. Chow and K. W. Cheung, "A toolbox for power system dynamics and control engineering education and research," *IEEE transactions on Power Systems*, vol. 7, no. 4, pp. 1559–1564, 1992.